

## ON THE CHOICE OF ESTIMATORS FOR USE WITH UNIVERSAL DETECTOR RESPONSE FUNCTIONS

**James Tickner\***  
CSIRO Minerals  
PMB 5, Menai, NSW 2234, Australia  
james.tickner@csiro.au

### ABSTRACT

Detector response functions (DRFs) are widely used in Monte Carlo simulations where it is necessary to estimate pulse-height spectra from physical detectors. Universal DRFs that can be used in a wide variety of problems are highly desirable. It is shown that the appropriate choice of tally estimator can considerably reduce the dependence of the DRF on the spatial and angular distribution of radiation incident on the detector. A new tally type, the interaction estimator, is developed which is found to be superior to traditional flux and current estimators for detector response problems. Efficient forms of flux, current and interaction estimators are developed for simulations where the detector volume is small compared to the total geometry size. An example application is presented and discussed.

*Key Words:* Response Functions, Response Matrix, Flux Estimator, Current Estimator

### 1 INTRODUCTION

A widely used variance reduction technique in problems where the responses of physical detectors are to be estimated is to separate the simulation into two parts. Firstly, particles from the radiation source are tracked through the problem geometry and the natures and energies of all particles striking the detector volume are recorded. Secondly, a detector response function is used to estimate the response of the detector to the incident radiation. The detector response function may come from a separate simulation or may be determined experimentally.

It is necessary to select an estimator to tally the particles striking the detector volume. Given the effort involved in obtaining a detector response function, it is desirable that the estimator-response function combination for a given detector should be reusable in a wide range of problems. In particular, the detector response should be accurately predicted irrespective of the direction and spatial distribution of the incident radiation.

Following Berger and Seltzer [1], the response function of a detector  $R(E_0, h)$  can be written as the convolution of an energy deposition spectrum  $D(E_0, E)$  and a resolution function  $G(E, h)$  multiplied by the detection efficiency  $\eta(E_0)$ :

$$R(E_0, h) = \eta(E_0) \int_0^{E_0} D(E_0, E) G(E, h) dE \quad (1)$$

where  $R(E_0, h)dh$  is the probability that a particle incident with energy  $E_0$  will produce a pulse

---

\* Tel. +61 2 9710 6732, Fax. +61 2 9710 6789

with height in the range  $h$  to  $h+dh$ ,  $\eta(E_0)$  is the probability that the incident particle interacts in the detector volume,  $D(E_0, E)dE$  is the probability that an interacting particle deposits an energy between  $E$  and  $E+dE$  and  $G(E, h)dh$  is the probability that the deposition of energy  $E$  will give rise to a pulse height between  $h$  and  $h+dh$ <sup>1</sup>.

Restricting the discussion from this point to neutral incident radiation, each of the functions  $\eta(E_0)$ ,  $D(E_0, E)$  and  $G(E, h)$  can depend on the angular and spatial distribution of the particles incident on the detector. The detector efficiency  $\eta$  depends on the thickness of material traversed. Particles interacting near the centre of the detector typically deposit a larger fraction of their energy than particles interacting near the edge. Non-uniform collection of light (from scintillators) or charge (from semi-conductor detectors) can lead to a spatial dependence of the resolution function  $G$ . All of these dependencies lead to  $R$  being problem-dependent.

This paper looks at ways to factor out as much of the spatial and angular dependence from  $R$  as possible. The suitability of widely used flux (or fluence) and current estimators for use with detector response functions is examined. A new tally type, termed the *interaction estimator* is developed, of which flux and current estimators are limiting cases. Efficient flux, current and interaction estimators are developed which are particularly suited for problems, often encountered in practice, where the detector dimensions are small compared to the overall size of the problem geometry.

## 2 SPATIAL AND ANGULAR DEPENDENCIES IN DETECTOR RESPONSE COMPONENT FUNCTIONS

The factors appearing on the right hand side of equation (1) depend in different ways on the spatial and angular distribution of radiation striking the detector volume. The radiation field at the detector can be specified in terms of the number of particles  $n(E_0, \mathbf{x}, \theta, \phi)$  with energy  $E_0$ , traveling in a direction  $(\theta, \phi)$  with respect to an arbitrary axis striking the detector surface at point  $\mathbf{x}$ . To illustrate the range in response variation, two specific cases will be considered for a cylindrical detector:

- Uncollimated, parallel beam incident over the entire visible surface of detector
- Ideally collimated, pencil beam directed at centre of detector volume.

In both cases, the detector response is evaluated as a function of the angle between the beam direction and the axis of the cylinder.

### 2.1 Detector Efficiency, $\eta$

The detector efficiency,  $\eta$ , is defined as the probability that a particle incident on the surface of the detector interacts inside the detector volume. For a uniform cylindrical volume, the detector efficiency can be calculated analytically for the two cases.

---

<sup>1</sup> For some detectors, the pulse height depends not only on the total energy deposited but also on the nature of the particles depositing the energy. The deposited energy  $E$  then needs to be replaced by some effective energy  $E^*$  for the factorization given in equation (1) to apply. For a non-linear scintillator, for example, light-yield would be a suitable quantity.

For an uncollimated, parallel beam of monochromatic radiation incident at an angle  $\theta$  to the axis of a detector with radius  $r$  and height  $h$ , the efficiency is given by [2]

$$\eta = 2(\pi r^2 \cos \theta + 2hr \sin \theta)^{-1} \times \left\{ 2hrb \sin \theta + [1 - \exp(-\mu h / \cos \theta)] \cdot \{ r^2 \cos \theta [\sin^{-1} b + b(1 - b^2)^{1/2}] - hr b \sin \theta - (br / \mu) \sin 2\theta \} + r(h \sin \theta - \sin 2\theta / \mu) \left( 1 - b - \int_b^1 \exp[-2\mu r (1 - x^2)^{1/2} / \sin \theta] dx \right) + r^2 \cos \theta \left( \pi / 2 - \sin^{-1} b - b(1 - b^2)^{1/2} + 2 \int_b^1 (1 - x^2)^{1/2} \exp[-2\mu r (1 - x^2)^{1/2} / \sin \theta] dx \right) \right\} \quad (2)$$

where  $b = [1 - (h/2r)^2 \tan^2 \theta]^{1/2}$  if  $(h/2r) \tan \theta < 1$  and 0 otherwise and  $\mu$  is the macroscopic cross-section. Equation (2) can be simplified for the limiting cases of low and high energy.

For low energy radiation where  $\mu h \gg 1$  and  $\mu r \gg 1$ , the efficiency reduces to  $\eta \approx 1$  – that is, every particle which hits the cylinder surface is detected. The response per unit flux is then just given by the projected cross-sectional area of the detector,  $A = 2hr \sin \theta + \pi r^2 \cos \theta$ . In the high energy limit, where  $\mu h \ll 1$  and  $\mu r \ll 1$  the efficiency is given by  $\pi r^2 \mu h / A$  and the response per unit flux by  $\pi r^2 \mu h = \mu V$  where  $V$  is the scintillator volume.

For a collimated pencil beam aimed at the centre of the detector, the efficiency is given by

$$\begin{aligned} \eta &= 1 - \exp(-2\mu r / \sin \theta) \text{ if } (h/2r) \tan \theta \geq 1 \\ \eta &= 1 - \exp(-\mu h / \cos \theta) \text{ if } (h/2r) \tan \theta < 1 \end{aligned} \quad (3)$$

In the low energy limit, the efficiency again reduces to  $\eta \approx 1$  and the response per unit flux is  $V \cos \theta / 2r$  if  $(h/2r) \tan \theta < 1$  and  $V \sin \theta / h$  otherwise. In the high energy limit, the efficiency is  $2\mu r / \cos \theta$  if  $(h/2r) \tan \theta < 1$  and  $\mu h / \sin \theta$  otherwise and the response per unit flux is  $\mu V$ .

As an example, figure 1 plots the calculated efficiencies for a “square” ( $h=2r$ ) cylindrical detector as a function of  $\theta$  for various values of  $\mu h$  in the range 0.25-12.

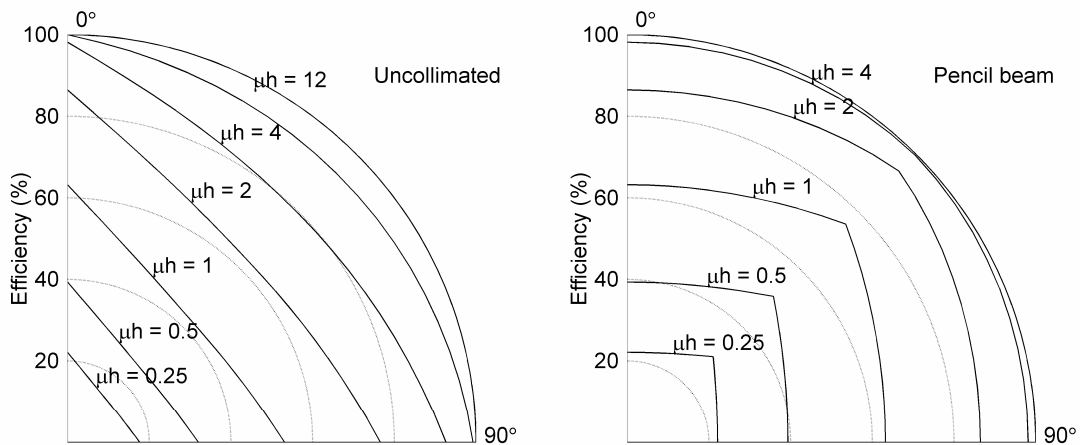


**Figure 1. Calculated efficiencies for a cylindrical detector ( $h=2r$ ) as a function of  $\theta$  and the product  $\mu h$  for uncollimated and collimated radiation beams.**

The left-hand plot shows the results for an uncollimated radiation beam calculated using equation (2). The right-hand plot shows the results for an ideally collimated pencil beam, calculated from equation (3). In both cases, the efficiency tends to 1 in the low-energy limit, but varies strongly with both angle of incidence and collimation at higher energies.

## 2.2 Energy Deposition Function, $D$

The calculation of the energy deposition function  $D(E_0, E)$  cannot in general be performed analytically, although approximate calculations can be made for certain geometries [3]. However, a Monte Carlo approach is more convenient. To investigate the effects on the energy deposition function  $D$  of the spatial and angular distribution of incident radiation, a simple MC simulation was performed using the EGSnrc [4] code. Monoenergetic gamma-rays, with energies variously chosen in the range 0.05 – 1.5 MeV were directed towards “square” (height  $h = 2 * \text{radius } r$ ) cylindrical NaI detectors with  $h = 1, 2, 4, \text{ or } 8$  cm. The energy deposited in the scintillator volume was tallied for approximately 6M events for each source energy/detector size combination.

The energy deposition function  $D(E_0, E)$  comprises several components, namely a full-energy peak, a photoelectric escape peak, a continuum due to singly or multiply Compton scattered gamma-rays and, for the highest energy gamma-rays, single and double annihilation gamma-ray escape peaks. The photofraction, or ratio of the full energy peak to the total area under the response curve, was chosen as a single parameter measure of the shape of  $D$ . Figure 2 plots the variation in the photofraction versus energy for 4 detector sizes.

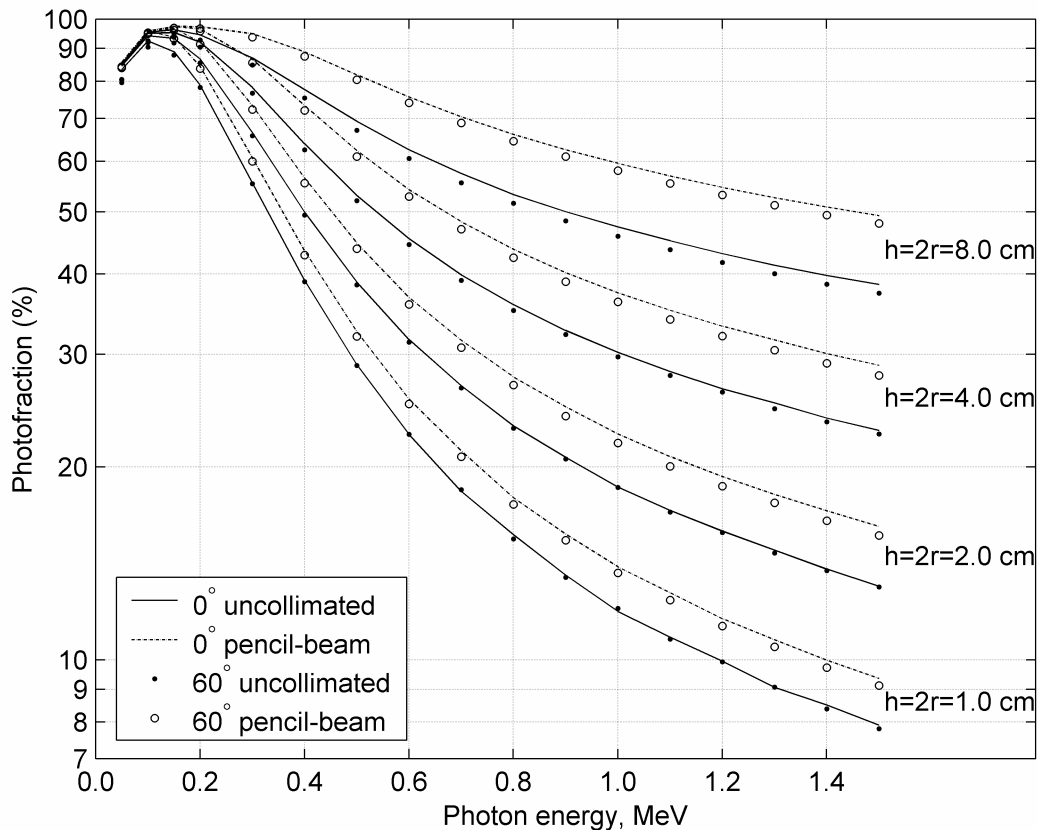


Figure 2. Photofraction as a function of energy for gamma-rays incident on a cylindrical detector.

For each detector size, 4 cases are shown, with collimated or uncollimated gamma-rays incident at  $0^\circ$  or  $60^\circ$  to the detector axis. The photofraction decreases with increasing energy and the greatest differences between the 4 cases are observed at the highest energy studied. For all detector sizes, the photofraction shows a strong dependence on the *collimation* of the incident radiation but is only weakly dependent on the direction of incidence. At 1.5 MeV, the photofraction for tightly collimated radiation is 17-28% higher than for radiation incident over the entire detector. However at the same energy, the photofraction for both pencil beam and uncollimated radiation at  $0^\circ$  angle of incidence is only 0.5-3% higher than the same cases at  $60^\circ$ .

### 2.3 Pulse Height Function, $G$

The pulse height function,  $G$ , does not normally depend on (high-energy) radiation transport processes and so cannot be calculated using the methods applied to ionizing radiation transport. The pulse height function reflects the atomic, optical and electronic processes used to convert the energy deposited in the detector into a measurable signal, which include light (scintillator) or charge (semiconductor detector) production, detection and amplification.

For a well designed detector,  $G$  is independent of where the radiation interacts and its direction of incidence. If it were otherwise, the energy resolution of the detector would be impaired. For example, for scintillator detectors, care is taken to ensure that the detection of scintillation photons is uniform through the crystal volume. For semiconductor detectors, charge collection is usually uniform away from the immediate surface of the detector.

An important exception is the class of anisotropic organic scintillators such as anthracene, where the light output depends on the direction of the incident radiation. This leads to a direction dependence in  $G$ , or in the energy deposition function  $D$  if the anisotropy is absorbed into an effective deposited energy  $E^*$  - see footnote 1.

## 3 THE INTERACTION TALLY ESTIMATOR

The results of the previous section can be summarized as follows. Of the three factors appearing in the response function definition equation (1):

- The efficiency,  $\eta$ , depends on both the spatial and angular distributions of radiation incident on the detector
- The energy deposition function,  $D$ , depends on whether the radiation is collimated or is incident over the entire detector surface, but depends only weakly on the direction of incidence
- The pulse height function,  $G$ , is largely independent of the spatial and angular distribution of incident radiation for many detector types

In practice, the collimation of many detectors is fixed by their construction. For example, large scintillation detectors used to measure neutron induced gamma-rays are usually unshielded and respond to radiation incident from all directions, whereas low-energy, high-resolution semiconductor X-ray detectors typically only respond to radiation incident over a narrow range of angles defined by the location of the detector with respect to an entrance window. The majority of the variation in the angular and spatial dependence of the response function,  $R$ , then enters through the efficiency.

To factor as much of this dependence from  $R$  as possible, it is therefore desirable to construct a tally  $T$  that measures the product of the number of particles incident on the detector (current) with the probability of their interacting. Such a tally counts the number of primary or initial interactions made by particles incident on the detector volume.

In the low-energy limit where the detector size is large compared to the interaction length of the incident radiation,  $\eta \rightarrow 1$  and every particle that enters the detector volume interacts. Consequently the tally  $T$  reduces to a simple current tally, counting the particles that enter the detector volume.

In the high energy limit where the radiation is highly penetrating, the probability of a particle interacting when it traverses the detector is given by  $\mu L$  where  $\mu$  is the macroscopic cross-section and  $L$  is the length of the particle's track through the detector. The quantity  $L/V$  where  $V$  is the detector volume is just the analogue track-length estimator of the average flux inside the detector, so  $T$  reduces to a simple flux tally, multiplied by  $\mu V$ .

The same low- and high-energy limits were deduced for the specific case of parallel radiation incident on a cylindrical detector in the previous section but are shown here to be generally true. Current and flux estimators are widely available in most general purpose Monte Carlo codes and are straightforward to program in custom-written codes, which perhaps accounts for their widespread use in detector response function simulation.

However, these estimators are optimal only in the limiting cases. One method for estimating  $T$  would be to directly count the number of primary interactions made by particles entering the detector volume. Only the first interaction made by any particle after entering the volume is included. A more efficient approach is to tally the quantity

$$T = 1 - \exp(-\mu L) \quad (4)$$

for each particle that enters the detector volume. In its simplest form, the interaction estimator is then an analogue, track-length current estimator with individual contributions weighted according to equation (4).

#### 4 EFFICIENT FLUX, CURRENT AND INTERACTION ESTIMATORS FOR SMALL DETECTORS

A significant disadvantage of the analogue flux, current and interaction estimators described in the previous section is their inefficiency. Only particles that actually enter the detector volume make a tally contribution. For problems where the detectors occupy only a small fraction of the total volume most particle histories are wasted.

The next-event point-flux estimator for neutral particles is well known [5]. Contributions to the flux estimator are made when a particle is created at the source and at each point where it undergoes a collision. The flux contribution at point  $\mathbf{x}_d$  due to a particle creation or collision event at point  $\mathbf{x}$  is given by

$$\phi = \frac{w e^{-\Sigma}}{r^2} \cdot \frac{dp}{d\Omega} \quad (5)$$

where  $w$  is the particle's weight,  $\Sigma = \int_0^r \mu(r') dr'$  is the integrated cross-section along the straight-

line path from  $\mathbf{x}$  to  $\mathbf{x}_d$ ,  $r = |\mathbf{x} - \mathbf{x}_d|$  is the distance between the creation/collision and detector positions and  $\frac{d\phi}{d\Omega}$  is the angular differential probability distribution for the source or scattered particle. For example, for an isotropic source producing particles with unit weight, equation (5) reduces to the familiar result  $\phi = e^{-\Sigma} / 4\pi r^2$ .

The point-flux estimator can be extended to calculate average volume fluxes, surface currents and interaction rates. The average flux inside some volume  $V$  is given by

$$\bar{\phi} = \int_V \phi dV \quad (6)$$

so the volume-averaged flux can be estimated by randomly sampling the detector position  $\mathbf{x}_d$  uniformly inside  $V$  before applying equation (5).

The current,  $j$ , entering volume  $V$  is given by

$$j = \int_{S'} \phi \cos \theta dA \quad (7)$$

where  $\theta$  is the angle between a particle's direction vector and the inward-pointing normal of the surface of  $V$  at the point where the particle enters,  $dA$  is an element of the surface and  $S'$  is the portion of the surface of  $V$  which is visible from the source/collision point  $\mathbf{x}$ . For a convex volume filled with a material with zero cross-section (vacuum), every particle enters and leaves exactly once. An alternative expression for  $j$  is then

$$j = \frac{1}{2} \int_S \phi |\cos \theta| dA \quad (8)$$

where  $S$  is the whole surface of  $V$ . The contribution of an event to the current of particles entering  $V$  is then given by  $\frac{1}{2} |\cos \theta| A \phi$  where  $A$  is the area of  $S$  and  $\phi$  is evaluated using equation (5) with the point  $\mathbf{x}_d$  sampled at random on  $S$ , uniformly with respect to area. In evaluating  $\Sigma$ , the cross-section of the material inside  $V$  is set to zero.

The extension to calculating the interaction rate is straightforward. The contribution of an event to the interaction rate tally  $T$  is given by

$$T = j \cdot [1 - e^{-\mu L}] = \frac{1}{2} |\cos \theta| A \phi \cdot [1 - e^{-\mu L}] \quad (9)$$

where, as before,  $\phi$  is evaluated using equation (5) with the point  $\mathbf{x}_d$  sampled at random on  $S$  and the cross-section of the material inside  $V$  set to zero. Here  $L$  is distance between the two points on  $S$  that lie on the line (possibly extended) connecting  $\mathbf{x}$  to  $\mathbf{x}_d$ .

## 5 EXAMPLE APPLICATIONS

To illustrate the use of the interaction tally estimator, a simple model of a gamma-gamma borehole logging probe is considered. The probe comprises a 10 mCi  $^{60}\text{Co}$  gamma-ray source, a 40 mm diameter  $\times$  60 mm long cylindrical tungsten shield and a 25 mm diameter  $\times$  75 mm long cylindrical NaI(Tl) arranged coaxially. The probe is situated in the centre of a 50 mm diameter

cylindrical hole passing through the centre of a large block of sand (composition  $\text{SiO}_2$ , density  $1.5 \text{ gcm}^{-3}$ ). The simulation aims to measure the response or pulse-height spectrum in the sodium iodide detector.

To provide a benchmark result, the pulse-height spectrum is calculated directly using an analogue energy-deposition tally with 150 bins equally spaced from 0 to 1.5 MeV. The energy spectrum of gamma-rays entering the detector volume is also measured using analogue flux (track-length), current (surface-crossing) and interaction estimators.

For the flux estimator, the material inside the detector volume has to be set to vacuum to avoid double counting of gamma-ray interactions inside the detector when the flux is folded with the detector response function. This is not required for the current or interaction estimators as these both count particles when they first enter the detector volume and are unaffected by subsequent interactions that the particle may undergo.

The detector response function is estimated using a separate simulation. A point source of gamma-rays is situated on the axis of the  $25 \times 75 \text{ mm}$  detector, 250 mm from the centre of the end face. Gamma-rays with a flat energy spectrum between 0 and 1.5 MeV are emitted over a range of polar angles just sufficient to illuminate the end face of the detector. The detector response is recorded in a  $150 \times 150$  element matrix with equally spaced, 10 keV wide energy binning. The column and row in which an event is tallied are chosen according to the deposited energy and the original energy of the source particle respectively. Let  $D(i,j)$  be the probability that a source particle with energy in the  $i^{\text{th}}$  row deposits an energy that places the event in the  $j^{\text{th}}$  column. The energy deposition matrices for use with flux, current and interaction estimators are then given by:

$$\begin{aligned} D_{FLUX}(i, j) &= D(i, j) / \bar{\phi} \\ D_{CURRENT}(i, j) &= D(i, j) / \bar{j} \\ D_{INTERACTION}(i, j) &= D(i, j) / \sum_j D(i, j) \end{aligned} \quad (10)$$

where  $\bar{\phi} = 0.1567 \text{ cm}^{-2}$  is the average flux per source particle inside the detector volume, measured when it contains a vacuum and  $\bar{j} = 1.0$  is the average current entering the detector per source particle. The replacement of the detector material with vacuum in the estimation of the average flux  $\bar{\phi}$  has to be made so that the normalization of  $D_{FLUX}$  matches the normalization assumed in the main borehole simulation.

The final detector responses,  $r$ , for the 4 different estimators are then given by

$$\begin{aligned} r_{DIRECT} &= t_{DIRECT} \cdot G \\ r_X &= (t_X \cdot D_X) \cdot G \end{aligned} \quad (11)$$

where  $t_{DIRECT}$  is the energy deposition spectrum measured using the direct, deposited energy estimator and  $t_X$  ( $X=FLUX$ ,  $CURRENT$  or  $INTERACTION$ ) are the spectra of gamma-rays entering the detector measured using the flux, current or interaction estimators respectively. The pulse height function  $G$  is represented by a  $150 \times 150$  matrix and simulates the finite energy resolution of the detector. The energy resolution was chosen to be Gaussian, with a full-width half-maximum of 8% at 662 keV and varying like  $E^{1/2}$ .

Figure 3 plots the 4 calculated detector responses. As expected, the current estimator response (dot-dash line) agrees well with the directly calculated response (open circles) at low energy whereas the flux estimator response (dashed line) agrees best for high-energy, highly penetrating gamma-rays. At low energies where the gamma-rays are strongly absorbed, the flux estimator underestimates the deposited energy spectrum. In the borehole model where gamma-rays are primarily incident on the side of the detector, the response per unit flux is higher than that predicted by the response function simulation where the gamma-rays are incident on the end of the detector. Similarly, the current estimator overestimates the response at high energies as the response per unit current for side-incident gamma-rays in the borehole model is lower than that for end-incident gamma-rays in the response function model. In contrast, the interaction estimator response (solid line) is in excellent agreement with the directly calculated response over the entire energy range.

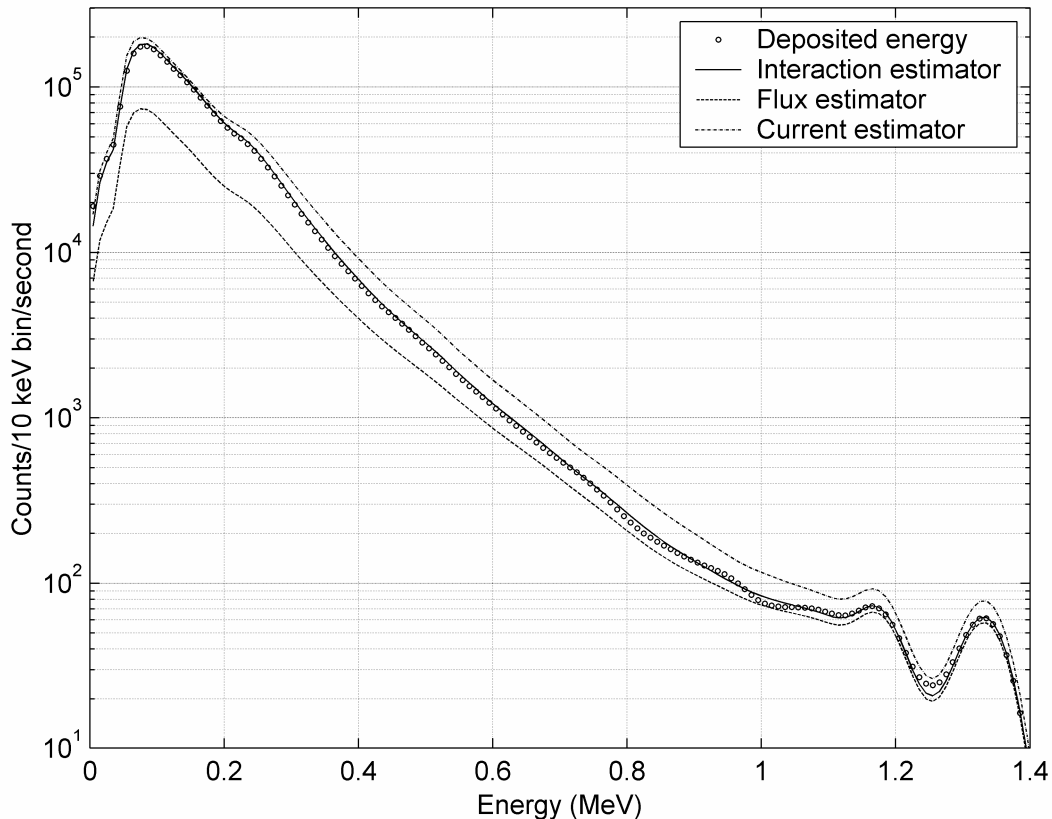


**Figure 3. Comparison of borehole detector response functions calculated using deposited energy (circles), interaction (solid line), flux (dot-dash line) and current (dashed line) estimators.**

To compare performances of the analogue interaction estimator, given by equation (4) and the next-event based estimator given by equation (9), separate runs of the borehole problem were performed using each estimator in term. A figure-of-merit given by  $FOM = (te_i^2)^{-1}$  was calculated for each of the 150 energy bins where  $t$  is the CPU time used in the run and  $e_i$  is the fractional statistical error in bin  $i$ . A doubling in the figure of merit corresponds to a halving of the time required to achieve a particular statistical accuracy. At the peak of the measured spectrum, around 0.1 MeV, the FOM for the next-event based interaction estimator is 3.0 times that of the analogue estimator. As the energy increases, the FOM ratio increases as increasingly rare, large-angle Rayleigh scatters are needed to reflect the source gamma-rays back into the detector. The

FOM ratios at 0.5, 1.0 and 1.33 MeV are 7.2, 21 and 43 respectively. For problems with proportionately smaller detector volumes, the FOM improvement is expected to be larger.

## 6 DISCUSSION AND CONCLUSIONS

The variation in the response of scintillator and semiconductor detectors with the spatial and angular distribution of incident radiation has been briefly reviewed. This variation is important when a Monte Carlo problem is factored into two pieces, one calculating the energy spectrum of particles arriving at a detector and the other determining the detector response function. Whilst a pulse-height or deposited energy spectrum can be calculated directly in some problems, factorizing out the detector response function has several advantages:

- The detector response may not be calculable using the Monte Carlo code in question. For example, highly non-analogue neutron transport codes such as MCNP cannot be used directly to calculate neutron response functions [6].
- There may be substantial efficiency gains for two reasons. Firstly, by convoluting the detected particle energy spectrum with a response matrix, the detector response is applied analytically rather than stochastically sampled. Secondly, a wider range of variance reduction methods is generally available for Monte Carlo problems that do not include non-Boltzmann (energy deposition) tallies.
- Experimental data, semi- or fully analytical methods and other, none Monte Carlo techniques can be used in the calculation of the detector response function – see for example [7] and references therein.

For weakly penetrating radiation, the response per unit *current* of particles entering the detector is most independent of the incident radiation direction. For high-energy penetrating radiation, the response per unit *flux* of particles through the detector is the most constant. Current and flux tally estimators are available in most general purpose Monte Carlo codes and are widely used in problems simulating detector responses. However, neither estimator is ideal and for accurate results it is necessary to ensure that the spatial and angular distribution of radiation incident on the detector used in the response function calculation matches that of the actual problem being simulated.

A new tally type, termed the interaction estimator, has been demonstrated. By factoring the detector efficiency out of the response function, the response function's sensitivity to variations in the direction of incident radiation is greatly reduced. Two variations on the response function estimator are presented, based on straightforward extensions to conventional analogue track-length and next-event flux estimators. The latter estimator is particularly suitable for problems with small detectors where the probability of radiation hitting the detector is low. In a sample problem, the detector response estimated using an interaction estimator is found to be substantially more accurate than those calculated using either current or flux tallies.

## 7 REFERENCES

1. M. J. Berger and S. M. Seltzer, "Response Functions for Sodium Iodide Scintillation Detectors," *Nucl. Instr. Meth*, **104**, pp. 317-332 (1972).

2. I. Petr, A. Adams and J. B. Birks, "Directional Characteristics of Cylindrical Scintillators," *Nucl. Instr. Meth*, **95**, pp. 253-257 (1971).
3. R. Muller and D. Maeder, "Single Crystal Spectroscopy", *Scintillation Spectroscopy of Gamma Radiation Vol 1*, Gordon and Breach, New York (1967).
4. I. Kawrakow and D. W. O. Rogers, "The EGSnrc Code System: Monte Carlo Simulation of Electron and Photon Transport," *NRCC Report*, **PIRS-701**
5. M. H. Kalos, "On the estimation of flux at a point by Monte Carlo," *Nucl. Sci. Eng.*, **16**, pp. 111-117 (1963).
6. J. R. Tickner, "Modelling Detector Responses to Neutrons Using MCNP," *Advanced Monte Carlo for Radiation Physics, Particle Transport Simulation and Applications (Proceedings of the Monte Carlo 2000 Conference)*, Lisbon, 23-26 October 2000, pp. 669-674.
7. A. Sood and R. P. Gardner, "A new Monte Carlo assisted approach to detector response functions," *Nucl. Instr. Meth. B*, **213**, pp. 100-104 (2004).